Industrial Crops & Products 223 (2025) 120199

Contents lists available at ScienceDirect

Industrial Crops & Products

journal homepage: www.elsevier.com/locate/indcrop

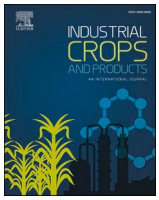

Biofilm inhibition and eradication activity of citral and borneol against foodborne bacteria

Wen Wang [a,b,c,d], Tom Coenye [c], Jianyu Su [b,d,*], Sheng-Xiang Qiu [a,**]

[a] Program for Natural Product Chemical Biology, State Key Laboratory of Plant Diversity and Specialty Crops, South China Botanical Garden, Chinese Academy of Sciences, Guangzhou, Guangdong 510650, China
[b] School of Food Science and Engineering, South China University of Technology, Guangzhou, Guangdong 510640, China
[c] Laboratory of Pharmaceutical Microbiology, Ghent University, Ghent, Belgium
[d] Sino-Singapore International Joint Research Institute, Guangzhou, Guangdong 510700, China

ARTICLE INFO

Keywords:
Foodborne bacteria
Biofilm inhibition and eradication
Membrane damage

ABSTRACT

Biofilms growing on food surfaces, packaging, equipment and processing environments bring huge risks to food safety and result in economic losses. Natural components are receiving increasing interest as "green" antimicrobial agents due to their biocompatibility, broad-spectrum antimicrobial properties, and antibiofilm potential. As a traditional adjuvant in Chinese medicine, borneol has the potential to enhance citral's antibiofilm efficacy. In this study, the antibiofilm activities of citral, borneol, and the combination citral and borneol (BC) against various foodborne bacteria were evaluated using multiple techniques. Light microscopy, crystal violet (CV) staining, and the 2,3-bis (2-methoxy-4-nitro-5-sulfophenyl)-5-[(phenylaminocarbonyl]-2H-tetrazolium hydroxide (XTT) assay were employed to monitor biofilm formation. Additionally, biofilm eradication was assessed against *Staphylococcus aureus* and *Escherichia coli* biofilms grown on polycarbonate membranes. Protein leakage was measured, and field emission scanning electron microscopy (FESEM) was used to examine cell membrane integrity. Results showed that borneol and citral acted synergistically to inhibit biofilms. Borneol, citral, alone or together inhibited biofilm formation in a concentration dependent manner, and they have the ability to inactivate or kill at least 90.7 ± 1.9 % bacteria in preformed biofilms. Both borneol and citral disrupted the membrane integrity of the bacteria, increased permeability, and ultimately led to cell death. These findings suggest that the combination citral and borneol has the potential to be developed as a food preservative or bactericidal agent for controlling foodborne bacterial contamination.

1. Introduction

Food products can be easily contaminated by a variety of pathogenic or spoilage microorganisms during processing, packaging, storage and transportation (De Filippis et al., 2021; Khan et al., 2024; Snyder et al., 2024). As a leading human opportunistic pathogen, *Pseudomonas aeruginosa* is frequently found in tap/drinking water, milk/dairy products, poultry/bovine meat, fish and plant-origin food (Xu et al., 2019). *Listeria monocytogenes* is notorious in ready-to-eat and minimally processed food due to its ability to multiply at refrigeration temperature (Vidovic et al., 2024). Furthermore, *Staphylococcus aureus* and *Escherichia coli* are the main reason for food poisoning (Argudín et al., 2010; Braz et al., 2024). Generally, bacteria tend to form mono-microbial and polymicrobial aggregates on interfaces or in liquids rather than exist as single and independent cells, commonly referred to as biofilms (Lv et al., 2023). Once biofilm formed, bacteria within biofilms becomes very resistant to disinfection processes due to low permeability to antibacterial agents.

In recent years, the trends in food processing are focusing on the use of natural compounds as antibacterial agents. It has been confirmed that natural components extracted from different essential oils (EOs) have broad-spectrum antimicrobial properties (He et al., 2022). Furthermore, many EOs and their extracts are classified as Generally Recognized as Safe (GRAS) by the US Food and Drug Administration (FDA) due to their high efficiency, safety and chemical diversity (Dima and Dima, 2015).

Borneol, a natural and lipophilic monoterpenoid compound with unique chiral characteristics, is primarily used as an adjuvant in

* Correspondence to: School of Food Science and Engineering, South China University of Technology, Wu Shan Road 381, Guangzhou 510640, China.
** Correspondence to: South China Botanical Garden, Chinese Academy of Sciences, Guangzhou, Guangdong 510650, China.
E-mail addresses: jysu@scut.edu.cn (J. Su), sxqiu@scbg.ac.cn (S.-X. Qiu).

https://doi.org/10.1016/j.indcrop.2024.120199
Received 22 September 2024; Received in revised form 26 November 2024; Accepted 2 December 2024
Available online 4 December 2024

traditional Chinese medicine formulations of centrally acting drug (Kulkarni et al., 2021). It's also confirmed that borneol have the ability to prevent bacterial adhesion (Ahmed et al., 2018; Cheng et al., 2021). Citral, a monoterpene aldehyde, is the predominant component of *Litsea cubeba* EO (Thielmann and Muranyi, 2019). Previous studies have shown that citral have good bacteriostatic activity against many foodborne pathogenic bacteria including *S. aureus*, *E. coli*, and *L. monocytogenes* (Ju et al., 2020). The potential application of citral has so far been studied for the preservation of fruit, vegetables, milk, juice, bread, and meat products, and as antimicrobial compound in food packaging films (Angane et al., 2022; Hartatie et al., 2019; Ju et al., 2020; Li et al., 2022; Prakash et al., 2020; Valková et al., 2022). However, one of the major problems in the application of citral to food matrices is the need for higher concentration. One possible solution is combining components that act synergistically to decrease the total concentrations needed (Bassolé and Juliani, 2012; Souza et al., 2022). The synergistic antibacterial activity of borneol and citral against Gram-positive and Gram-negative foodborne bacteria, including *P. aeruginosa*, *E. coli*, *S. aureus*, and *L. monocytogenes* in their planktonic forms has been demonstrated in author's previous study (Wang et al., 2021). However, till now there are no reports regarding the synergistic antibiofilm activity of the combination borneol and citral, their potential application in food industry, not even to elucidate their antibiofilm mechanism.

In this study, the antibiofilm activities of citral, borneol, and the combination citral and borneol (BC) against various foodborne bacteria were evaluated using multiple techniques. Based on contact surfaces of bacteria in real-world food environment, polystyrene surface, polycarbonate membrane, and glass surface were hired to serve as substrate material for bacterial adherence. Subsequently, leakage of intracellular protein and morphologic change of bacteria in biofilms were studied to elucidate the mechanism of action. The ultimate purpose is to provide effective data for exploring antibiofilm activities of citral and borneol, and more accurately predict their potential applications.

2. Materials and methods

2.1. Materials, bacterial strains, and culture conditions

Borneol (≥98 % purity) was supplied by Guangdong Huaqingyuan Biological Technology Co., Ltd (Meizhou, China). Citral (98 % purity) and absolute ethanol were obtained from Aladdin Biochemical Technology Co., Ltd (Shanghai, China). Trypticase soy broth (TSB) and trypticase soy agar (TSA) were obtained from Guangdong Huankai Microbial Technology Co., Ltd (Guangzhou, China). The following bacterial strains were used: *P. aeruginosa* ATCC 27853, *E. coli* ATCC 43894, *L. monocytogenes* ATCC 19118 and *S. aureus* ATCC 23235. Bacteria strains were routinely stored at −80℃ and were grown on TSA or in TSB at 37°C, under aerobic conditions. All experiments were conducted using Milli-Q water.

2.2. Biofilm inhibition assay

Considering the maximum solubility of borneol in citral, BC was prepared by dissolving the hydrophobic solid borneol into citral at a mass ratio of 1:4 (Wang et al., 2022). Minimal inhibitory concentration (MIC) values of borneol, citral, and BC were also obtained in author's previous study (Wang et al., 2021). Stock solutions of borneol, citral and BC (100 mg/mL in 60 % sterile ethanol) were prepared and diluted to the required concentrations with sterile TSB firstly. Then, a 2-fold dilution series of these components were prepared in the sterile 96-well microtiter plate (100 μL/well), producing a concentration range from 1/64 × MIC to 8 × MIC. Bacterial suspension with a density of approximately 1×10^6 CFU/mL was prepared by diluting the log-phase bacterial cultures into TSB. Finally, 100 μL of this suspension was added to 96-well plates together with the above diluted antimicrobial agent. The total volume in each well of the above system was 200 μL. One well with sterile medium served as blank control, while another well containing inoculum (5×10^5 CFU/mL) was used as positive control. Cultures were incubated statically at 37℃ for 6 h, 12 h, 24 h, and 48 h, respectively. All experiments were conducted in at least triplicate.

Biofilm biomass was quantified using the crystal violet (CV) staining method (Feoktistova et al., 2016; Xu et al., 2016). After incubation, the supernatants were discarded, and the plates were washed three times with 200 μL sterile phosphate buffered saline (PBS). The biofilms were then fixed with 70 % ethanol for 20 min. Following the ethanol was removed and 100 μL of 0.01 % CV solution was added to each well. After 15 min, the excess CV was rinsed away with sterile PBS twice. Finally, the fixed CV was released by washing with 95 % ethanol. A volume of 125 μL of the solution was transferred to a new 96-well microtiter plate, and the absorbance was measured at 540 nm. One well containing sterile medium served as the blank control. All procedures were performed at room temperature.

The modified XTT (2,3-bis [2-methyloxy-4-nitro-5-sulfophenyl]-2H-tetrazolium-5-carboxanilide) method (Bao et al., 2017; Du et al., 2012) was used to evaluate biofilm viability. After incubation, the plates were washed three times with sterile PBS and dried in a reversal position. Then 100 μL PBS and 100 μL XTT-menadione solution (Promega Corporation, US) were added to each prewashed well. Plates were covered with aluminum foil and incubated for 2 h at 37℃. Absorbance was measured at 490 nm using an ELISA plate reader with a fresh 96-well plate.

2.3. Biofilm eradication assay

The biofilm eradication effect of test compounds was assessed using the CFU counting method. In brief, log-phase bacterial cultures were inoculated on a polycarbonate membrane placed in the center of a TSA plate and incubated at 37℃, allowing biofilm formation for 24, 48, 72, 96, 120, 144 and 168 h, respectively. To ensure adequate nutrient supply, the biofilms were transferred to fresh TSA plates every two days. The established biofilms on the polycarbonate membranes were then treated with 2 × MIC solutions (5 mL in TSB medium) for 4 h. Inoculums without test compounds served as the control groups. The remaining bacteria were detached from the polycarbonate membranes using a sonicator (125 W, 20 kHz, 5 s on/5 s off, repeated 3 times), and CFU counts was determined by plating. The biofilm eradication rate (%) was calculated using the following formula:

$$\text{Biofilm eradication rate}(\%) = \frac{\text{CFU}_{control} - \text{CFU}_{treatnent}}{\text{CFU}_{control}} \times 100$$

2.4. Quantification of protein leakage

To quantify intracellular leakage from bacteria within biofilms, 1 mL of the above bacterial suspension was centrifuged at 5000 × g for 5 min. The total soluble protein concentration in the supernatant was measured using the Bradford method (Moragues-Saitua et al., 2019; Yang et al., 2019) with a Bradford Protein Assay Kit (Beyotime, Shanghai, China). Bacterial suspension from biofilms treated with the same volume of TSB medium were used as controls. Protein leakage was calculated as the difference between the total extracellular protein content in the experimental group and the control group. Different concentrations (0.025, 0.05, 0.1, 0.2, 0.3, 0.4 and 0.5 mg/mL) of bovine serum albumin (Beyotime, Shanghai, China) were prepared as standards. Sample absorbance at 562 nm was measured in a 96-well plate using a Tecan Infinite M200 plate reader (Tecan Trading Co., Ltd., Männedorf, Switzerland). The standard curve is shown in Fig. S1.

2.5. Field emission scanning electron microscopy (FESEM) observation

Biofilm eradication on round glass sheets (10 mm of diameter) was

investigated using a 24-well microtiter plate. Established biofilms (48 h) were treated in each well with 1 × MIC stock solutions for 4 h. While wells without the test compounds served as controls. After treatment, the solutions were discarded, and the glass sheets were thoroughly washed with PBS to remove unbound cells. The adhering cells were then fixed with 2.5 % glutaraldehyde. Following fixation, the glass sheets were dehydrated, washed with a gradient of ethanol, and air-dried at room temperature. Morphological changes of bacteria within biofilms were observed using a field emission scanning electron microscope (JEOL, Tokyo, Japan).

2.6. Statistical analysis

All experiments were conducted in biological triplicates (with at least three technical replicates for each biological sample, i.e., $n \geq 3 \times 3$) and are expressed as means ± standard deviations (SDs). Statistical analysis was performed using GraphPad Prism 7.0 software (GraphPad Prism version 7.00; GraphPad Software, La Jolla, CA, USA). To analyze the variance and determine significant differences between the means, a one-way analysis of variance (ANOVA) was conducted. Comparisons between multiple factors were performed using two-way ANOVA. Significant differences between means were assessed using the Tukey's test. Statistical significance was evaluated at the 95 % confidence level.

3. Results and discussion

3.1. Biofilm formation and biofilm inhibition on polystyrene surface

The time course of biofilm formation by four common bacteria, *L. monocytogenes*, *P. aeruginosa*, *E. coli*, and *S. aureus*, on the polystyrene surface were assessed. The total biofilm mass was highly correlated with the CV dye's binding ability to the extracellular polymeric substances (EPS) and both live and dead bacterial cells (Pipattanachat et al., 2021; Rodríguez-Melcón et al., 2021). CV staining indicated increasing biofilm formation 4–48 h (Fig. 1).

Next, biofilm inhibition activity of borneol, citral, and BC at different concentrations was evaluated by determining the total biofilm biomass (CV, OD_{540}) and biofilm viability (XTT, OD_{490}). For *L. monocytogenes* (Fig. 2A–C), the total biofilm mass steadily increased with incubation time in the control group (untreated). *L. monocytogenes* demonstrated the ability to adhere on the polystyrene surface and form biofilms within 6 h. Biofilm biomass grew rapidly between 6 h and12h, then slowed after 12 h, peaking at 48 h. Previous studies also confirmed that *L. monocytogenes* could attach to glass slides within 3 h and form biofilms within 24 h (Chae and Schraft, 2000). When co-incubation with borneol, citral or BC at the concentration of 1 × MIC or higher, no biofilm formation was detected on the polystyrene surface (Fig. 2). In contrast to biofilm biomass, biofilm viability increased steadily from 6 h to 24 h, peaking at 24 h before decreasing to a minimum at 48 h (Fig. 2D–F), which correlated closely with the growth stage of *L. monocytogenes* (Fernández et al., 1997). Biofilms lost their proliferation activity when the concentration of the tested components exceeded 1 × MIC, indicating that all tested components inhibited biofilm formation. Notably, BC at lower concentrations exhibited superior biofilm inhibition activity against *L. monocytogenes* compared to citral alone. While the antibacterial effect of borneol against *L. monocytogenes* has been demonstrated by several researchers (Mourey and Canillac, 2002), reports on its antibiofilm effect, apart from author's previous studies, are scarce.

For *E. coli*, both biofilm mass and viability increased with longer incubation times, while higher concentrations of test components led to decreased biofilm mass and reduced viability (Fig. 3). For *P. aeruginosa* and *S. aureus* (Figs. 4–5), the OD_{540} values were obviously bigger than the other 2 strains at the concentrations of lower than 1 × MIC, suggesting stronger biofilm formation abilities of these two strains. Once the bacterial cells attached to the polystyrene surface, dense and smooth biofilms quickly established, which can effectively reduce the penetration of effective antimicrobial agents into the biofilm, thus reducing the antimicrobial effect. While at the concentrations higher than 1 × MIC, borneol, citral, or BC reduced the OD_{540} values to approximately zero, and thus prevented all four strain to develop biofilms. Biofilm viability is directly proportional to the number of active cells within the biofilms. As

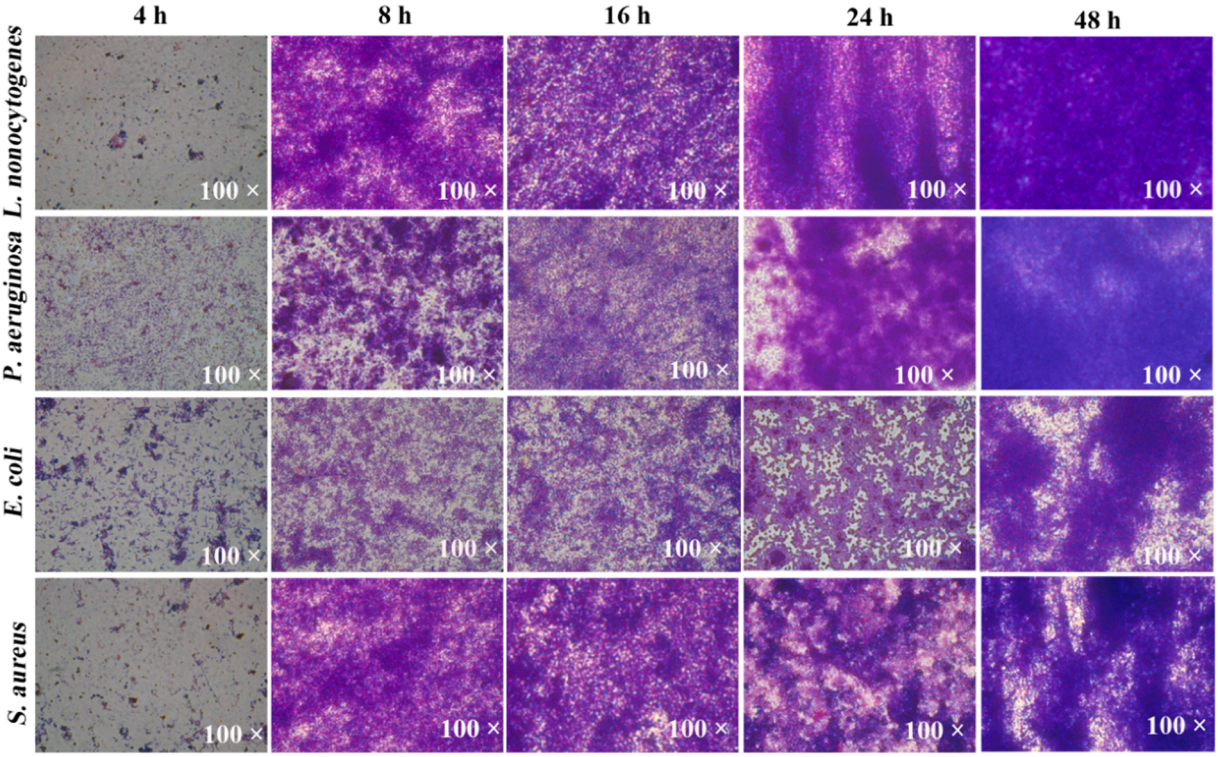

Fig. 1. Dynamic of biofilm growth on polystyrene surface stained by crystal violet at different time point.

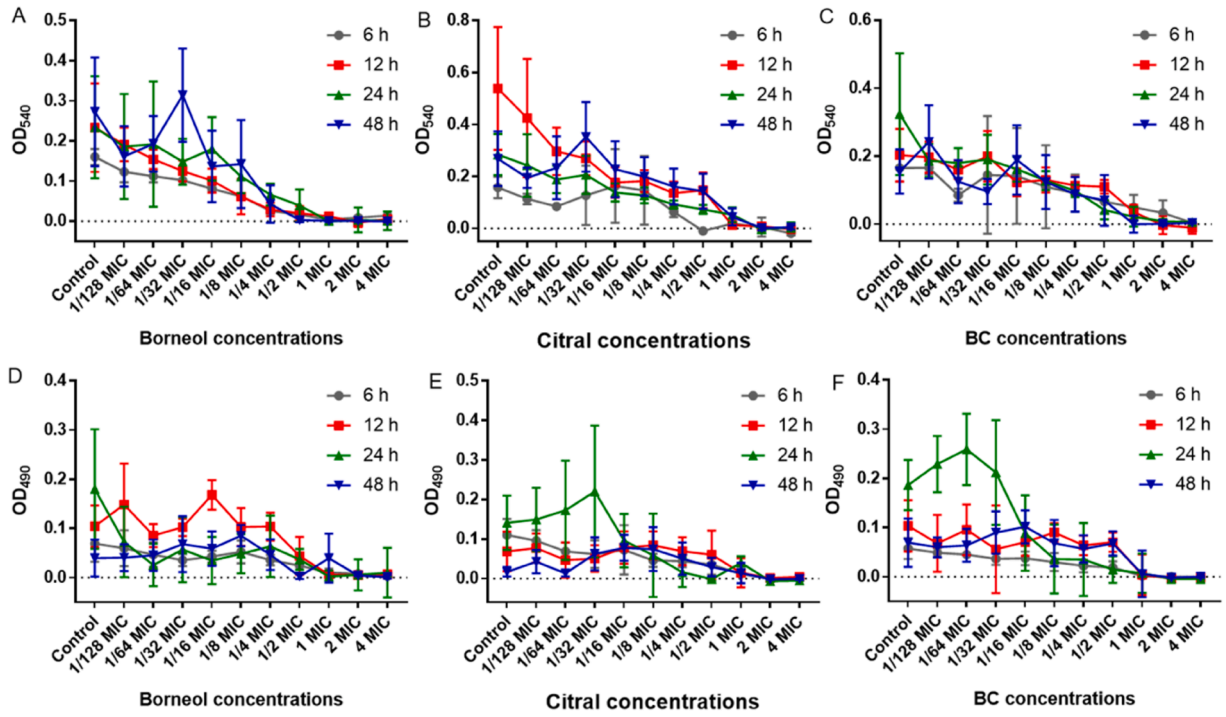

Fig. 2. The inhibitory effects of tested compounds on *L. monocytogenes* biofilm formation. Biofilm mass (OD_{540}) was determined by crystal violet assay (A-C) and biofilm viability (OD_{490}) was determined by XTT assay (D-F). Data are reported as mean ± standard deviation of three independent experiments ($n \geq 9$).

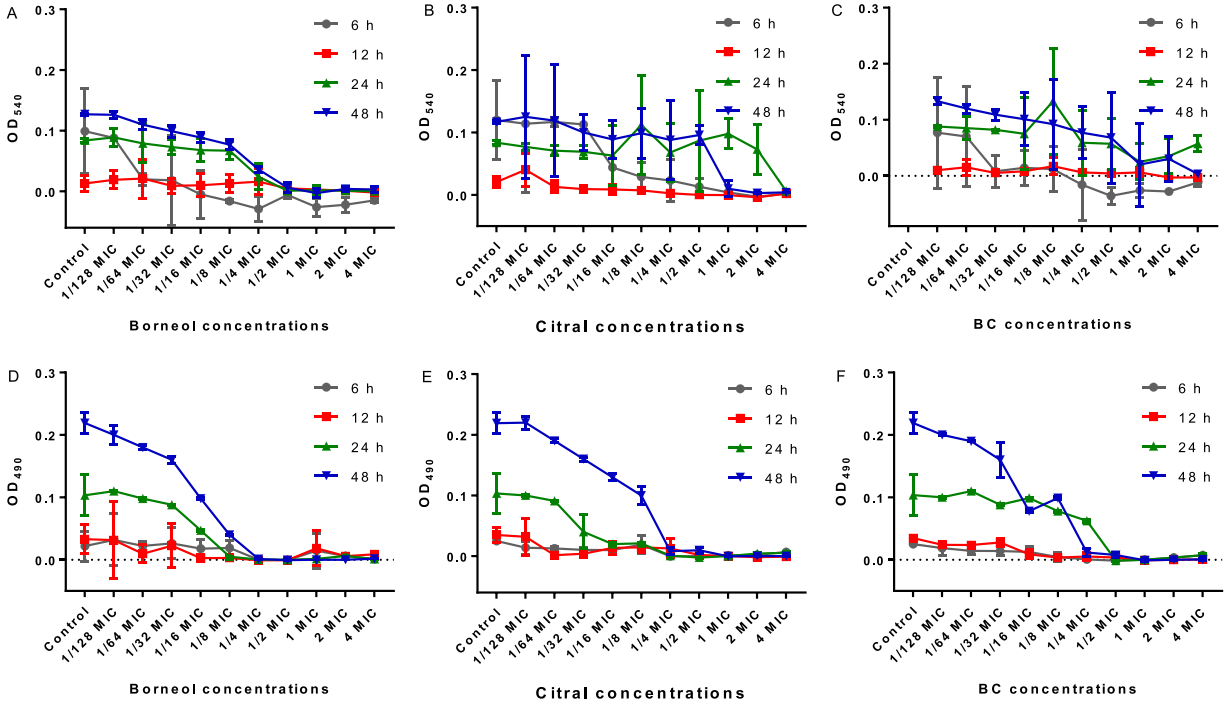

Fig. 3. The inhibitory effects of tested compounds on *E. coli* biofilm formation. Biofilm mass (OD_{540}) was determined by crystal violet assay (A-C) and biofilm viability (OD_{490}) was determined by XTT assay (D-F). Data are reported as mean ± standard deviation of three independent experiments ($n \geq 9$).

the concentration of test compounds increases, the metabolic tendency of bacterial cells gradually decreased. These findings demonstrated that borneol, citral, alone or together inhibited biofilm formation in a concentration dependent manner. Similar to *L. monocytogenes*, BC also have better biofilm inhibition activities against the other three bacteria compared to citral alone. These results clearly revealed the synergistic antibiofilm activities of these two components. The above result was same with other researchers that the inhibitory effect on biofilm formation by borneol was concentration dependent and correlated with its stereochemical structure, and borneol reduced biofilm formation mainly by inhibiting the initial step of eversible adhesion through chemotaxis recognition, involving both motor energy and intention (Cai et al., 2024; Sulaiman et al., 2022). In other study, borneol was also confirmed to improve the cellular uptake of other component by increasing cell

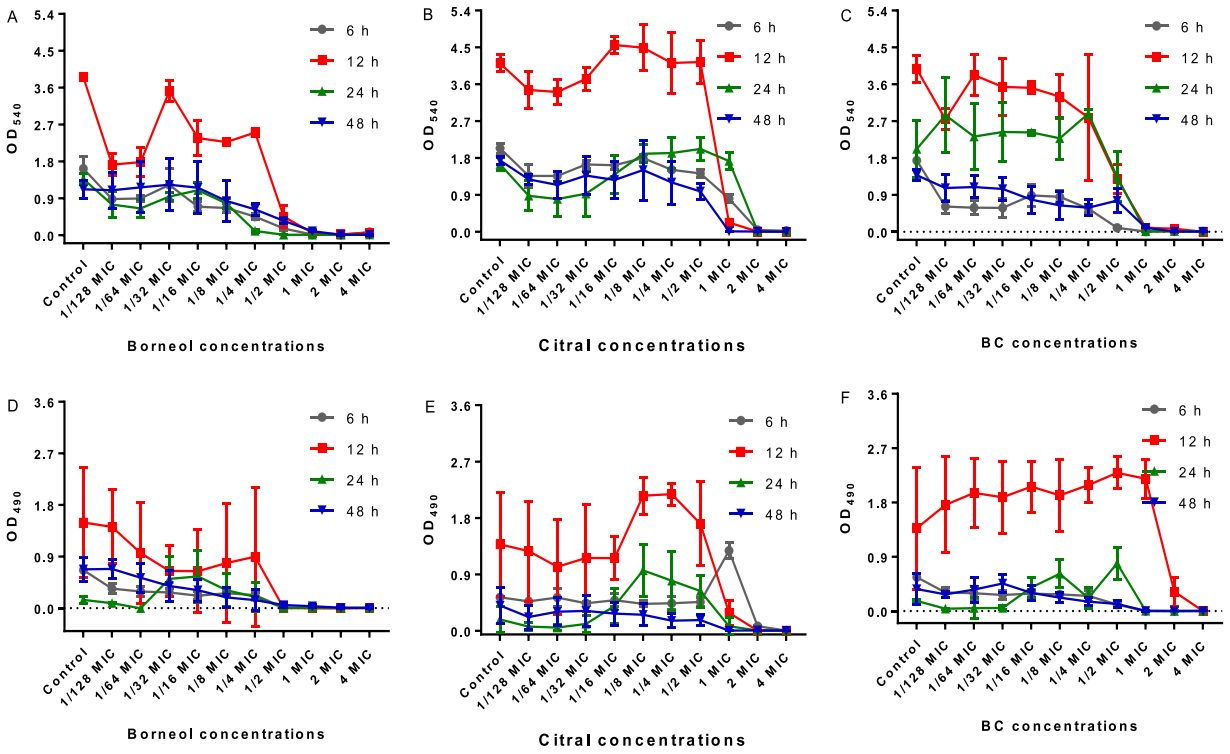

Fig. 4. The inhibitory effects of tested compounds on *P. aeruginosa* biofilm formation. Biofilm mass (OD_{540}) was determined by crystal violet assay (A-C) and biofilm viability (OD_{490}) was determined by XTT assay (D-F). Data are reported as mean ± standard deviation of three independent experiments ($n \geq 9$).

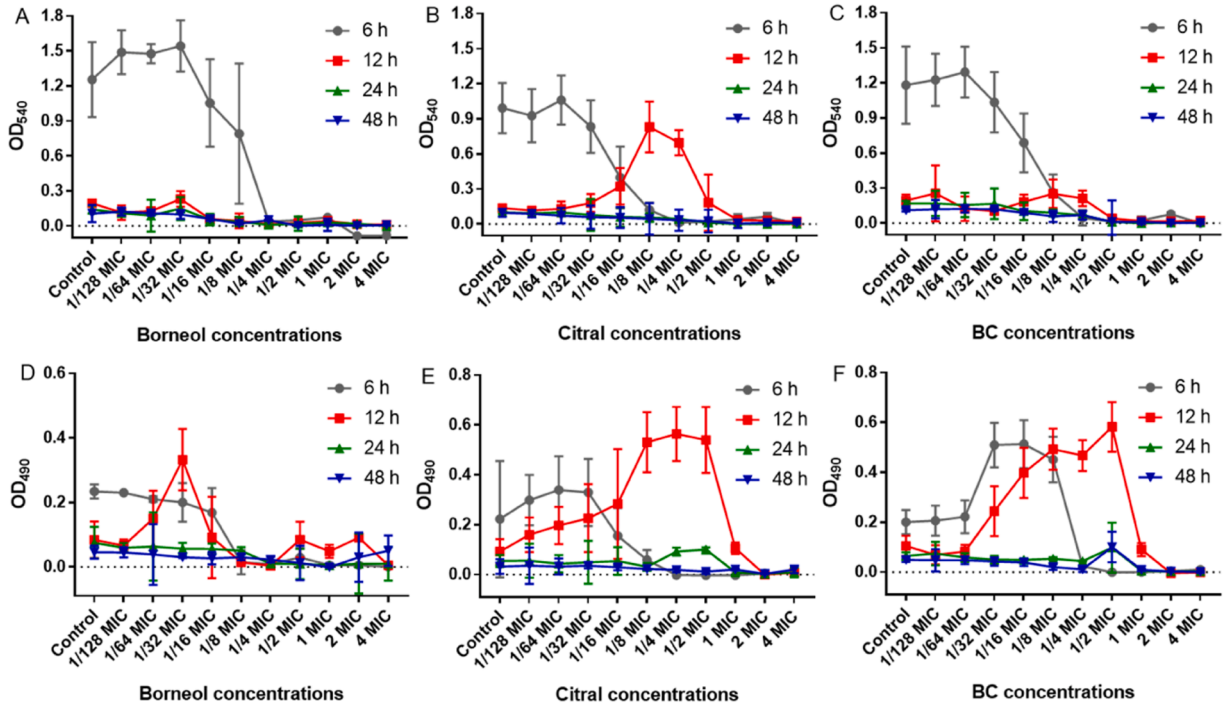

Fig. 5. The inhibitory effects of tested compounds on *S. aureus* biofilm formation. Biofilm mass (OD_{540}) was determined by crystal violet assay (A-C) and biofilm viability (OD_{490}) was determined by XTT assay (D-F). Data are reported as mean ± standard deviation of three independent experiments ($n \geq 9$).

permeability. As a result, the excessive accumulation of citral inside the cell triggered its death procedure.

The microtiter assay is usually used as a high throughput screening tool for antibacterial and anti-biofilm drugs (Shukla and Rao, 2017). However, substantial deviation commonly exists from experiment to experiment, and even from well to well, which normally caused by the method selected to remove the supernatant prior to CV staining or XTT reacting (i.e. pipetting or manually discarding the fluid by inversion, washed or unwashed wells) (Bozzini et al., 2023; Kragh et al., 2019). As shown in Fig. 2 to Fig. 5, substantial deviations were also observed in our

study. Therefore, more complex *in vitro* biofilm models were used to evaluate the biofilm eradication activities in the following experiment.

3.2. Biofilm eradication by borneol, citral, or BC on polycarbonate membrane

Two preformed biofilms of *E. coli* and *S. aureus* grown on polycarbonate membranes over 7 days (Fig. 6) were exposed to borneol, citral, or BC at the concentration of 2 × MIC for 4 h (Fig. 7). As shown in Fig. 7, in the initial adhesion stage, the number of viable bacteria recovered from 24 h preformed *S. aureus* biofilms appeared less ($P < 0.0001$) with very little EPS compared with the other preformed biofilms, while the maximum number of viable bacteria was found ($P < 0.05$) within 48 h preformed biofilm. Different from *S. aureus*, the maximum number of viable bacteria was achieved ($P < 0.05$) within 24 h preformed *E. coli* biofilm. Then the number of viable bacteria from older *S. aureus* biofilms (48–168 h) and *E. coli* biofilms (24–168 h) kept stable accompanied by more EPS formation. The 144h- and 168h-old *S. aureus* biofilms had the typical dry crystalline morphology. Bacteria within 120 h old *E. coli* biofilms even demonstrated twitching motility. It's known that bacterial flagellar motility plays an important role in many processes that occur at surfaces, including adhesion and biofilm formation (Laganenka et al., 2020).

In the biofilm eradication assay (Fig. 7), the number of culturable cells (CFU/membrane) recovered from preformed *S. aureus* and *E. coli* biofilms after 4 h exposure to test compounds at concentration of 2 × MIC showed a statistically significant ($P < 0.0001$) decrease compared with the untreated control. Furthermore, borneol, citral and BC inactivated almost all bacteria within test biofilms only except for a few time points. These time points included preformed *S. aureus* biofilms (48 h and 144 h) treated by borneol, citral, and BC, and preformed *E. coli* biofilms (24 h, 120 h and 168 h) treated by citral or BC. For untreated control at these time points, the number of culturable cells recovered from preformed biofilms was up to or higher than 10^9 CFU/mL, which were much larger than the experimental groups treated by test compounds (~10^3-10^7 CFU/membrane). These data with fluctuations also indicated that there is a need to improve these compounds' stabilities for better antibacterial effect. When examining their antibiofilm effects by calculating the bactericidal rate (Table 1), the test compounds inactivated or killed at least 90.7 ± 1.9 % bacteria in these preformed biofilms. All these data suggested that, borneol, citral and especially BC had powerful biofilm eradication activities against *S. aureus* and *E. coli.*

3.3. Preliminary investigation of the mechanisms behind the antibiofilm activity

3.3.1. Analysis of biofilm morphology

To visualize the interaction between bacterial cells and borneol, citral, or BC in biofilm, the biofilm eradication effect of these compounds was also studied using FESEM to observe the morphologic changes of *E. coli* and *S. aureus* biofilms formed on glass surface. Representative biofilm structures are shown in Fig. 8. In the control group, dense clusters of *E. coli* and multi-layer packs were observed, indicating that the untreated biofilm exhibited a compact architecture with a high density of viable cells. *E. coli* cells in the control group displayed intact, typical rod-shapes, and with no visible holes or morphologic change. The cell surface of *S. aureus* in control cells was smooth, complete, even, and typical hemispherical in shape. However, treatment with borneol, citral, and BC significantly disrupted the biofilm structure, leading to an increase in the number of dead cells The integrity of the cell membranes of both bacteria was progressively compromised. After 4 h of treatment with citral or borneol, sunken surfaces and hollow holes began to appear, with further damage observed following combination treatment. It was clearly revealed that the cell membrane of *E. coli* was pierced by citral, borneol or BC, possibly resulting in compromised bacterial membrane integrity, osmotic imbalance and bacterial death (Ahmed et al., 2020; Saleem et al., 2017). Similarly, the morphology of *S. aureus* cells treated with citral was altered and deformed (Fig. 8). These altered cells displayed wrinkled cell walls (due to citral treatment), micro-pores, and evidence of released intracellular compounds (following treatment with borneol or BC). Furthermore, the indistinguishable cellular contents seen in the treated cells, as captured in FESEM images, resembled denatured DNA and precipitated proteins, consistent with previous reports (Qian et al., 2020).

3.3.2. Protein leakage analysis

Protein leakage is considered as a representative indicator of cytoplasm leakage (Mao et al., 2019), cell injury and nonselective micropore formation (Tang et al., 2020). whether citral, borneol or BC can cause protein leakage in bacteria was investigated. After treated *S. aureus* biofilms with citral, borneol and BC at the concentration of 2 × MIC for 4 h, protein leakage was gradually increased between 24 h and 48 h (Fig. 9A), which is consistent with the increased cell death within biofilms (Fig. 7). The higher concentrations of protein leakage ($P < 0.05$) were observed from 96 h and 120 h old *S. aureus* biofilms, indicating that citral, borneol and BC promoted protein leakage of bacteria, which

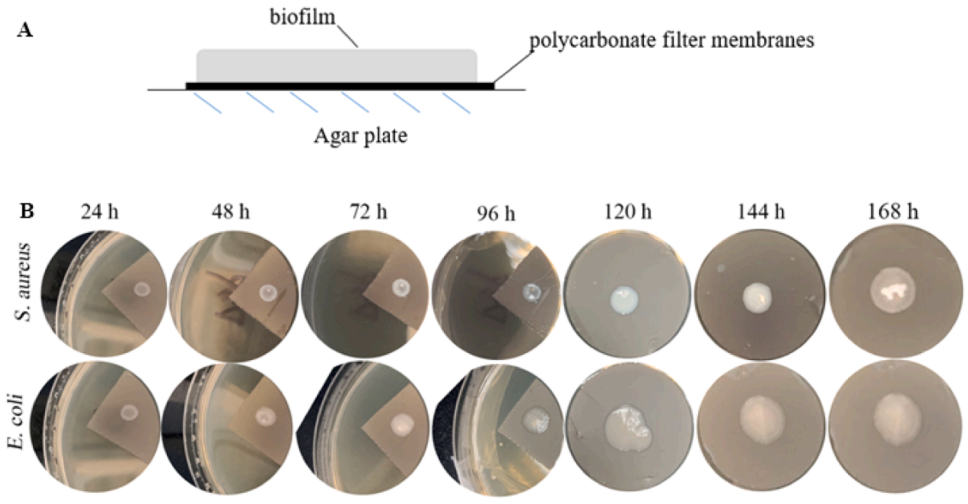

Fig. 6. Biofilm model on polycarbonate membrane (A) and morphology observation of different preformed biofilms grown on polycarbonate membranes in TSA for 24 h, 48 h, 72 h, 96 h, 120 h, 144 h and 168 h (B). All photomicrographs are shown at the same scale.

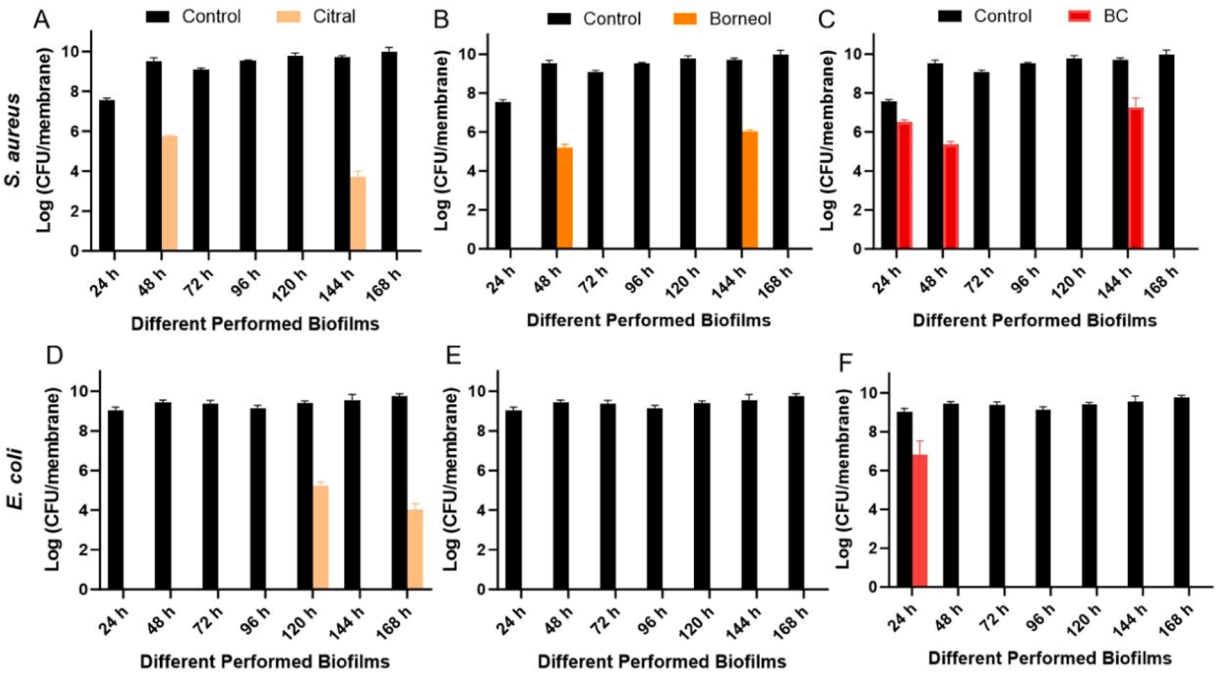

Fig. 7. Number of culturable cells (CFU/membrane) recovered from different preformed *S. aureus* and *E. coli* biofilms grown on polycarbonate membranes after 4 h exposure to compounds (Citral, Borneol and BC) at concentration of 2 × MIC (A and B).

Table 1
Biofilm eradication (%) of compounds at concentration of 2 × MIC on the different preformed *S. aureus* and *E. coli* biofilms on polycarbonate membranes after 4 h treatment compared with untreated control.

	Biofilms							
Strains	Components	24 h	48 h	72 h	96 h	120 h	144 h	168 h
S. aureus	Citral	100 ± 0.0[a]	100 ± 0.0	100 ± 0.0	100 ± 0.0	100 ± 0.0	100.0 ± 0.0	100 ± 0.0
	Borneol	100 ± 0.0[a]	100 ± 0.0	100 ± 0.0	100 ± 0.0	100 ± 0.0	100.0 ± 0.0	100 ± 0.0
	BC	90.7 ± 1.9[b]	100 ± 0.0	100 ± 0.0	100 ± 0.0	100 ± 0.0	99.7 ± 0.6	100 ± 0.0
E. coli	Citral	100 ± 0.0[a]	100 ± 0.0	100 ± 0.0	100 ± 0.0	100 ± 0.0	100 ± 0.0	100 ± 0.0
	Borneol	100 ± 0.0[a]	100 ± 0.0	100 ± 0.0	100 ± 0.0	100 ± 0.0	100 ± 0.0	100 ± 0.0
	BC	99.0 ± 0.8[b]	100 ± 0.0	100 ± 0.0	100 ± 0.0	100 ± 0.0	100 ± 0.0	100 ± 0.0

Data are reported as mean ± standard deviation of at least three independent experiments (n ≥ 3), and different letters indicate significant difference ($P < 0.001$). Significant differences between means were assessed using the Tukey's test.

should be ascribed to the severe disruption of the bacterial membrane (Fig. 9A). These antibacterial agents didn't markedly change the cell membrane of 72 h, 144 h and 168 h old biofilm bacteria. This may be due to insufficient penetration of antibacterial molecules or the high heterogeneity biofilms with high number of persister cells (De la Fuente-Núñez et al., 2013; Lebeaux et al., 2014).

For *E. coli* (Fig. 9B), the protein leakage caused by citral, borneol or BC between 24 h to 72 h old biofilm bacteria was similar to *S. aureus*, confirming that these antibacterial agents had indiscriminate membrane damage to Gram-negative and Gram-positive bacteria. However, the destruction of cell membranes within older *E. coli* biofilms (≥ 96 h) was limited. The possible reason is that the dense biofilm structures together with the persister cells on the top layer hindered the penetration of citral, borneol or BC and thus made them ineffective (Mah and O'Toole, 2001).

The protein leakage caused by citral, borneol or BC was consistent with cell damage observed by FESEM, thus further prove the membrane damage caused by citral, borneol or BC. Several procedures may be responsible for the preliminary mechanism of biofilm eradication effect: (1) firstly, borneol and citral attach to the surface of bacterial and mainly destroy the integrity of the cell membrane within biofilms; (2) Secondly, a large number of cytoplasm, including K^+, proteins, etc., leak out of the cell within biofilms; (3) cell gradually die within biofilm structure; (4) biofilm structures begin to collapse and finally biofilm eradication effect is achieved.

In total, polystyrene surface, polycarbonate membrane, and glass surface in this study were hired to serve as substrate material for bacterial adherence. Though excellent biofilm inhibition, biofilm eradication effects achieved as well as preliminary antibiofilm mechanism explored, there are difference between laboratory conditions and real-world food environment. For example, all the biofilm models in this study focused on mono-species cultures, whereas nearly all biofilm communities in nature contains multiple bacterial species, and clearly multispecies biofilms are different and more complex than monospecies biofilms. Therefore, direct extrapolations of results obtained from monoculture lab experiments to complex natural biofilms are therefore imprecise and sometimes misleading (Burmølle et al., 2014). There are also clear indications that food matrix, food contact surfaces (Teflon, stainless steel, glass, and polystyrene), environmental temperature and moisture affect the establishment of biofilms (Nkemngong and Teska, 2024). Hence, antibiofilm effects of citral and borneol in different real food environment still need to be further verified.

4. Conclusion

In the present study, biofilm formation of four bacterial strains on

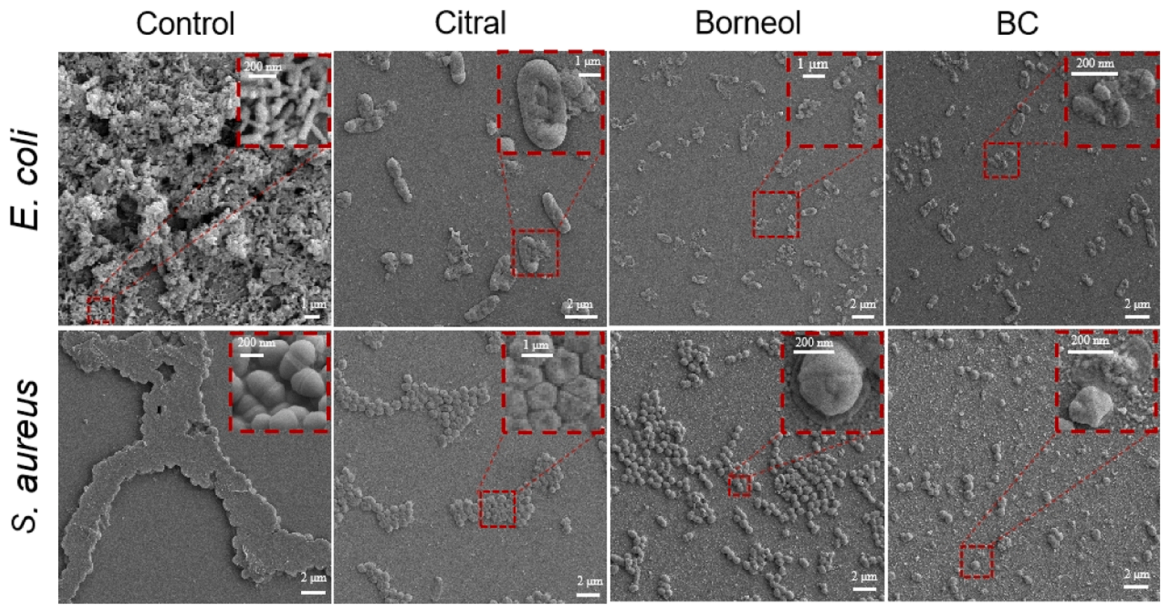

Fig. 8. Field emission scanning electron microscopy (FESEM) images of preformed biofilms (48 h) after 4 h treatment with 1 × MIC concentration of compounds.

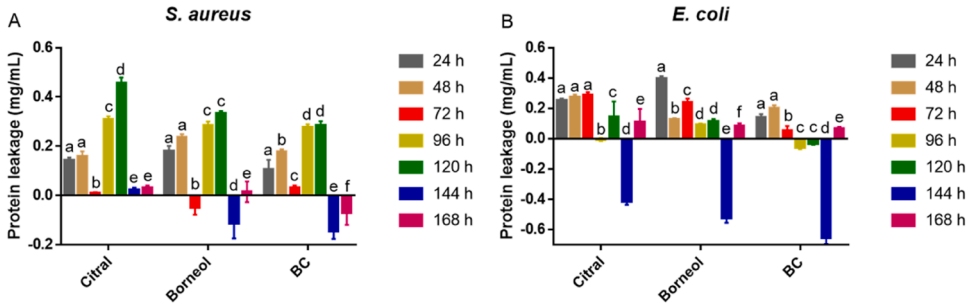

Fig. 9. Intracellular protein leakage from *S. aureus* and *E. coli* biofilm cells after 4 h treatment with 2 × MIC concentration of compounds. Biofilms treated with the same volume of TSB medium were used as negative control. Intracellular protein leakage was calculated by the difference between the total extracellular protein content in the experimental group and the total extracellular protein content in the negative control group. Data are reported as mean ± standard deviation of three independent experiments (n = 3). Letters represent significant differences ($P < 0.05$) between two adjacent data, which is obtained by two-way ANOVA followed by Tukey test.

polystyrene surface, as well as the biofilm eradication of two representative strains, *S. aureus* and *E. coli*, on polycarbonate membrane and glass surface were markedly achieved by borneol/citral/BC. Furthermore, borneol/citral/BC caused bacterial cell death through discrupting bacterial membrane, and subsequently leading to leakage of intracellular materials. The results highlight the importance of evaluating natural components in various models to more accurately predict their potential applications.

Funding information

This work was funded by the Postdoctoral Fellowship Program of China Postdoctoral Science Foundation under Grant Number GZC20232726 and Chinese Scholarship Council (CSC, NO. 319 202006150108). This work was also supported by the National Natural Science Foundation of China under Grant Number 32372449, the Basic and Applied Basic ResearchFoundation of Guangdong Province (2022A1515012196), and the Science and Technology Program of Meizhou (2021A0105001 and 2021A0107003).

CRediT authorship contribution statement

Jianyu Su: Writing – review & editing, Supervision, Resources, Project administration, Funding acquisition, Conceptualization. **Tom Coenye:** Writing – review & editing, Supervision, Resources. **Sheng-Xiang Qiu:** Supervision, Resources, Project administration. **Wen Wang:** Writing – review & editing, Writing – original draft, Software, Methodology, Investigation, Formal analysis, Data curation.

Declaration of Competing Interest

The authors declare no potential conflicts of interest.

Appendix A. Supporting information

Supplementary data associated with this article can be found in the online version at doi:10.1016/j.indcrop.2024.120199.

Data Availability

The data that has been used is confidential.

References

Ahmed, B., Ameen, F., Rizvi, A., Ali, K., Sonbol, H., Zaidi, A., Khan, M.S., Musarrat, J.J. Ao, 2020. Destruction of cell topography, morphology, membrane, inhibition of respiration, biofilm formation, and bioactive molecule production by nanoparticles

of Ag, ZnO, CuO, TiO2, and Al2O3 toward beneficial soil bacteria. ACS Omega 5, 7861–7876. https://doi.org/10.1021/acsomega.9b04084.
Ahmed, B., Hashmi, A., Khan, M.S., Musarrat, J., 2018. ROS mediated destruction of cell membrane, growth and biofilms of human bacterial pathogens by stable metallic AgNPs functionalized from bell pepper extract and quercetin. Adv. Powder Technol. 29, 1601–1616. https://doi.org/10.1016/j.apt.2018.03.025.
Angane, M., Swift, S., Huang, K., Butts, C.A., Quek, S.Y., 2022. Essential oils and their major components: an updated review on antimicrobial activities, mechanism of action and their potential application in the food industry. Foods 11, 464. https://doi.org/10.3390/foods11030464.
Argudín, M.Á., Mendoza, M.C., Rodicio, M.R.J.T., 2010. Food poisoning and Staphylococcus aureus enterotoxins. Toxins 2, 1751–1773. https://doi.org/10.3390/toxins2071751.
Bao, X., Jia, X., Chen, L., Peters, B.M., Lin, C.-w, Chen, D., Li, L., Li, B., Li, Y., Xu, Z., 2017. Effect of polymyxin resistance (pmr) on biofilm formation of Cronobacter sakazakii. Microb. Pathog. 106, 16–19. https://doi.org/10.1016/j.micpath.2016.12.012.
Bassolé, I.H.N., Juliani, H.R., 2012. Essential oils in combination and their antimicrobial properties. Molecules 17, 3989–4006. https://doi.org/10.3390/molecules17043989.
Bozzini, M.F., Pieracci, Y., Ascrizzi, R., Najar, B., D'Antraccoli, M., Ciampi, L., Peruzzi, L., Turchi, B., Pedonese, F., Alleva, A.J.F., 2023. Chemical composition and antimicrobial activity against the listeria monocytogenes of essential oils from seven salvia species. Foods 12, 4235. https://doi.org/10.1016/j.micpath.2020.104510.
Braz, M., Pereira, C., Freire, C.S., Almeida, A., 2024. Potential of bacteriophage phT4A as a biocontrol agent against Escherichia coli in food matrices. Int. J. Food Microbiol. 424, 110847. https://doi.org/10.1016/j.ijfoodmicro.2024.110847.
Burmølle, M., Ren, D., Bjarnsholt, T., Sørensen, S.J.J.Tim, 2014. Interactions in multispecies biofilms: do they actually matter? Trends Microbiol. 22, 84–91. https://doi.org/10.1016/j.tim.2013.12.004.
Chae, M.S., Schraft, H.J.Ijofm, 2000. Comparative evaluation of adhesion and biofilm formation of different Listeria monocytogenes strains. Int. J. Food Microbiol. 62, 103–111. https://doi.org/10.1016/S0168-1605(00)00406-2.
Cheng, Q., Asha, A.B., Liu, Y., Peng, Y.-Y., Diaz-Dussan, D., Shi, Z., Cui, Z., Narain, R., 2021. Antifouling and antibacterial polymer-coated surfaces based on the combined effect of zwitterions and the natural borneol. ACS Appl. Mater. Interfaces 13, 9006–9014. https://doi.org/10.1021/acsami.0c22658.
De Filippis, F., Valentino, V., Alvarez-Ordonez, A., Cotter, P.D., Ercolini, D., 2021. Environmental microbiome mapping as a strategy to improve quality and safety in the food industry. Curr. Opin. Food Sci. 38, 168–176. https://doi.org/10.1016/j.cofs.2020.11.012.
De la Fuente-Núñez, C., Reffuveille, F., Fernández, L., Hancock, R.E., 2013. Bacterial biofilm development as a multicellular adaptation: antibiotic resistance and new therapeutic strategies. Curr. Opin. Microbiol. 16, 580–589. https://doi.org/10.1016/j.mib.2013.06.013.
Dima, C., Dima, S., 2015. Essential oils in foods: extraction, stabilization, and toxicity. Curr. Opin. Food Sci. 5, 29–35. https://doi.org/10.1016/j.cofs.2015.07.003.
Du, X.-j, Wang, F., Lu, X., Rasco, B.A., Wang, S., 2012. Biochemical and genetic characteristics of Cronobacter sakazakii biofilm formation. Res. Microbiol. 163, 448–456. https://doi.org/10.1016/j.resmic.2012.06.002.
Feoktistova, M., Geserick, P., Leverkus, M., 2016. Crystal Violet Assay for Determining Viability of Cultured Cells. Cold Spring Harbor Protocols, 2016, pdb. prot087379. https://doi.org/10.1101/pdb.prot087379.
Fernández, P.S., George, S.M., Sills, C.C., Peck, M.W., 1997. Predictive model of the effect of CO2, pH, temperature and NaCl on the growth of Listeria monocytogenes. Int. J. Food Microbiol. 37, 37–45. https://doi.org/10.1016/S0168-1605(97)00043-3.
Hartatie, E.S., Prihartini, I., Widodo, W., Wahyudi, A., 2019. Bioactive compounds of Lemongrass (Cymbopogon citratus) essential oil from different parts of the plant and distillation methods as natural antioxidant in broiler meat. IOP Conf. Ser. Mater. Sci. Eng. https://doi.org/10.1088/1757-899X/532/1/012018.
He, R., Zhang, Z., Xu, L., Chen, W., Zhang, M., Zhong, Q., Chen, H., Chen, W., 2022. Antibacterial mechanism of linalool emulsion against Pseudomonas aeruginosa and its application to cold fresh beef. World J. Microbiol. Biotechnol. 38, 1–18. https://doi.org/10.1007/s11274-022-03233-4.
Ju, J., Xie, Y., Yu, H., Guo, Y., Cheng, Y., Zhang, R., Yao, W., 2020. Synergistic inhibition effect of citral and eugenol against Aspergillus niger and their application in bread preservation. Food Chem. 310, 125974. https://doi.org/10.1016/j.foodchem.2019.125974.
Khan, S., Monteiro, J.K., Prasad, A., Filipe, C.D., Li, Y., Didar, T.F., 2024. Material breakthroughs in smart food monitoring: intelligent packaging and on-site testing technologies for spoilage and contamination detection. Adv. Mater. 36, 2300875. https://doi.org/10.1002/adma.202300875.
Kragh, K.N., Alhede, M., Kvich, L., Bjarnsholt, T.J.B., 2019. Into the well—a close look at the complex structures of a microtiter biofilm and the crystal violet assay. Biofilm 1, 100006. https://doi.org/10.1016/j.bioflm.2019.100006.
Kulkarni, M., Sawant, N., Kolapkar, A., Huprikar, A., Desai, N., 2021. Borneol: a promising monoterpenoid in enhancing drug delivery across various physiological barriers. AAPS PharmSciTech 22, 1–17. https://doi.org/10.1208/s12249-021-01999-8.
Laganenka, L., López, M.E., Colin, R., Sourjik, V., 2020. Flagellum-mediated mechanosensing and RflP control motility state of pathogenic Escherichia coli. mBio 11, e02269–02219. https://doi.org/10.1128/mbio.02269-19.
Lebeaux, D., Ghigo, J.-M., Beloin, C., 2014. Biofilm-related infections: bridging the gap between clinical management and fundamental aspects of recalcitrance toward antibiotics. Microbiol. Mol. Biol. Rev. 78, 510–543. https://doi.org/10.1128/mmbr.00013-14.
Li, Y.-x, Erhunmwunsee, F., Liu, M., Yang, K., Zheng, W., Tian, J., 2022. Antimicrobial mechanisms of spice essential oils and application in food industry. Food Chem., 132312 https://doi.org/10.1016/j.foodchem.2022.132312.
Lv, X., Wang, L., Mei, A., Xu, Y., Ruan, X., Wang, W., Shao, J., Yang, D., Dong, X.J.S., 2023. Recent nanotechnologies to overcome the bacterial biofilm matrix barriers. Small 19, 2206220. https://doi.org/10.1002/smll.202206220.
Mah, T.-F.C., O'Toole, G.A., 2001. Mechanisms of biofilm resistance to antimicrobial agents. Trends Microbiol. 9, 34–39. https://doi.org/10.1016/S0966-842X(00)01913-2.
Mao, C., Xiang, Y., Liu, X., Zheng, Y., Yeung, K.W.K., Cui, Z., Yang, X., Li, Z., Liang, Y., Zhu, S., 2019. Local photothermal/photodynamic synergistic therapy by disrupting bacterial membrane to accelerate reactive oxygen species permeation and protein leakage. ACS Appl. Mater. Interfaces 11, 17902–17914. https://doi.org/10.1021/acsami.9b05787.
Moragues-Saitua, L., Merino-Martín, L., Stokes, A., Staunton, S., 2019. Towards meaningful quantification of glomalin-related soil protein (GRSP) taking account of interference in the Coomassie Blue (Bradford) assay. Eur. J. Soil Sci. 70, 727–735. https://doi.org/10.1111/ejss.12698.
Mourey, A., Canillac, N.J.Fc, 2002. Anti-Listeria monocytogenes activity of essential oils components of conifers. Food Control 13, 289–292. https://doi.org/10.1016/j.foodcont.2019.01.025.
Nkemngong, C., Teska, P.J.Fi.M., 2024. Biofilms, mobile genetic elements and the persistence of pathogens on environmental surfaces in healthcare and food processing environments. Front. Microbiol. 15, 1405428. https://doi.org/10.3389/fmicb.2024.1405428.
Pipattanachat, S., Qin, J., Rokaya, D., Thanyasrisung, P., Srimaneepong, V., 2021. Biofilm inhibition and bactericidal activity of NiTi alloy coated with graphene oxide/silver nanoparticles via electrophoretic deposition. Sci. Rep. 11, 1–9. https://doi.org/10.1038/s41598-021-92340-7.
Prakash, A., Baskaran, R., Vadivel, V., 2020. Citral nanoemulsion incorporated edible coating to extend the shelf life of fresh cut pineapples. LWT 118, 108851. https://doi.org/10.1016/j.lwt.2019.108851.
Qian, W., Zhang, J., Wang, W., Wang, T., Liu, M., Yang, M., Sun, Z., Li, X., Li, Y., 2020. Antimicrobial and antibiofilm activities of paeoniflorin against carbapenem-resistant Klebsiella pneumoniae. J. Appl. Microbiol. 128, 401–413. https://doi.org/10.1111/jam.14480.
Rodríguez-Melcón, C., Alonso-Hernando, A., Riesco-Peláez, F., García-Fernández, C., Alonso-Calleja, C., Capita, R., 2021. Biovolume and spatial distribution of foodborne Gram-negative and Gram-positive pathogenic bacteria in mono-and dual-species biofilms. Food Microbiol. 94, 103616. https://doi.org/10.1016/j.fm.2020.103616.
Saleem, S., Ahmed, B., Khan, M.S., Al-Shaeri, M., Musarrat, J.J.M.P., 2017. Inhibition of growth and biofilm formation of clinical bacterial isolates by NiO nanoparticles synthesized from Eucalyptus globulus plants. Microb. Pathog. 111, 375–387. https://doi.org/10.1016/j.micpath.2017.09.019.
Shukla, S.K., Rao, T.S.J.B., 2017. An improved crystal violet assay for biofilm quantification in 96-well microtitre plate. Biorxiv, 100214. https://doi.org/10.1101/100214.
Snyder, A.B., Martin, N., Wiedmann, M., 2024. Microbial food spoilage: impact, causative agents and control strategies. Nat. Rev. Microbiol. 1–15. https://doi.org/10.1038/s41579-024-01037-x.
Souza, V.V.M.A., Almeida, J.M., Barbosa, L.N., Silva, N.C.C., 2022. Citral, carvacrol, eugenol and thymol: antimicrobial activity and its application in food. J. Essent. Oil Res. 1–14. https://doi.org/10.1080/10412905.2022.2032422.
Tang, C., Chen, J., Zhang, L., Zhang, R., Zhang, S., Ye, S., Zhao, Z., Yang, D., 2020. Exploring the antibacterial mechanism of essential oils by membrane permeability, apoptosis and biofilm formation combination with proteomics analysis against methicillin-resistant Staphylococcus aureus. Int. J. Med. Microbiol. 310, 151435. https://doi.org/10.1016/j.ijmm.2020.151435.
Thielmann, J., Muranyi, P., 2019. Review on the chemical composition of Litsea cubeba essential oils and the bioactivity of its major constituents citral and limonene. J. Essent. Oil Res. 31, 361–378. https://doi.org/10.1080/10412905.2019.1611671.
Valková, V., Ďúranová, H., Galovičová, L., Borotová, P., Vukovic, N.L., Vukic, M., Kačániová, M., 2022. Cymbopogon citratus essential oil: its application as an antimicrobial agent in food preservation. Agronomy 12, 155. https://doi.org/10.3390/agronomy12010155.
Vidovic, S., Paturi, G., Gupta, S., Fletcher, G.C.J.CrifS., Nutrition, 2024. Lifestyle of Listeria monocytogenes and food safety: emerging listericidal technologies in the food industry. Crit. Rev. Food Sci. 64, 1817–1835. https://doi.org/10.1080/10408398.2022.2119205.
Wang, W., Bao, X., Bové, M., Rigole, P., Meng, X., Su, J., Coenye, T., 2022. Antibiofilm activities of borneol-citral-loaded Pickering emulsions against Pseudomonas aeruginosa and Staphylococcus aureus in physiologically relevant chronic infection models. Microbiol. Spectr. 10. https://doi.org/10.1128/spectrum.01696-22 e01696-01622.
Wang, W., Ren, Z., Wang, L., Cai, Y., Ma, H., Fang, L., Su, J., 2021. Nanoparticle-stabilized encapsulation of borneol and citral: Physicochemical characteristics, storage stability, and enhanced antibacterial activities. J. Food Sci. 86, 4554–4565. https://doi.org/10.1111/1750-3841.15910.

Xu, Z., Liang, Y., Lin, S., Chen, D., Li, B., Li, L., Deng, Y., 2016. Crystal violet and XTT assays on Staphylococcus aureus biofilm quantification. Curr. Microbiol. 73, 474–482. https://doi.org/10.1007/s00284-016-1081-1.

Xu, Z., Xie, J., Soteyome, T., Peters, B.M., Shirtliff, M.E., Liu, J., Harro, J.M.J.Coifs, 2019. Polymicrobial interaction and biofilms between Staphylococcus aureus and Pseudomonas aeruginosa: an underestimated concern in food safety. Curr. Opin. Food Sci. 26, 57–64. https://doi.org/10.1016/j.cofs.2019.03.006.

Yang, H., Hu, J., Lu, X., Wang, F., Shen, W., Hu, W., Wang, L., Chen, X., Liu, L., 2019. Improving extracellular protein production in Escherichia coli by overexpressing D, D-carboxypeptidase to perturb peptidoglycan network synthesis and structure. Appl. Microbiol. Biotechnol. 103, 793–806. https://doi.org/10.1007/s00253-018-9510-7.